Available online at www.sciencedirect.com
ScienceDirect
Trans. Nonferrous Met. Soc. China 30(2020) 484−491
Transactions of Nonferrous Metals Society of China
www.tnmsc.cn

Mechanism of sodium sulfide on flotation of cyanide-depressed pyrite

Zhao CAO[1,2,3], Peng WANG[1], Wen-bo ZHANG[1], Xiao-bo ZENG[4], Yong-dan CAO[1]

1. Institute of Mining Engineering, Inner Mongolia University of Science and Technology, Baotou 014010, China;
2. Guangdong Institute of Resources Comprehensive Utilization, Guangzhou 510650, China;
3. State Key Laboratory of Rare Metals Separation and Comprehensive Utilization, Guangzhou 510650, China;
4. Institute of Multipurpose Utilization of Mineral Resources, Chinese Academy of Geological Science, Chengdu 610041, China

Received 3 June 2019; accepted 19 November 2019

Abstract: The mechanism of sodium sulfide (Na_2S) on the flotation of cyanide-depressed pyrite using potassium amyl xanthate (PAX) as collector was investigated by flotation test and electrochemical measurements. The flotation results show that both PAX and Na_2S can promote the flotation recovery of cyanide-depressed pyrite and their combination can further improve the pyrite flotation recovery. Electrochemical measurements show that PAX and Na_2S interacted with cyanide-depressed pyrite through different mechanisms. PAX competed with cyanide and was adsorbed on the pyrite surface in the form of dixanthogen, thus enhancing the hydrophobicity and flotation of cyanide-depressed pyrite. Unlike PAX, Na_2S rendered the pyrite surface hydrophobic through the reduction of ferricyanide species and the formation of elemental sulfur S^0 and polysulfide S_n^{2-}. The combined application of PAX and Na_2S induced superior pyrite flotation recovery because of a synergistic effect between PAX and Na_2S.
Key words: pyrite; chalcocite; flotation; cyanide; depression; sodium sulfide

1 Introduction

Gold generally exists in most copper−gold ores as free gold, copper-associated gold and pyrite-associated gold, which are usually recovered by gravity separation and sequential flotation where copper-bearing minerals are first floated to a saleable copper−gold concentrate with pyrite to be depressed, and then the depressed pyrite is activated and floated to recover the associated gold [1,2]. Chalcopyrite and chalcocite widely exist as primary and secondary copper-bearing minerals, respectively, in most copper−gold ores. In the previous study, we found that the depressed pyrite in chalcopyrite flotation by lime could be floated by the addition of PAX (potassium amyl xanthate) or Na_2S through different mechanisms [3]. While the addition of PAX removed the hydrophilic metal oxidation species, followed by the adsorption of PAX on pyrite surface, the addition of Na_2S formed elemental sulfur and polysulfide on pyrite surface, both of which increase the hydrophobicity of pyrite [3].

However, the chalcocite-dominant copper ores are more difficult to treat because more copper ions emanate from chalcocite than from chalcopyrite to promote stronger copper activation on pyrite [4−6]. In this case, lime is not an efficient pyrite depressant and cyanide is often required to depress pyrite in copper flotation [7].

Different mechanisms have been proposed to

Foundation item: Project (51764045) supported by the National Natural Science Foundation of China; Project (NJYT-18-B08) supported by Inner Mongolia Young Science & Technology Talent Support Plan, China; Project (GK-201804) supported by Research Fund Program of State Key Laboratory of Rare Metals Separation and Comprehensive Utilization, China; Project (DD20190574) supported by China Geological Survey Project
Corresponding author: Xiao-bo ZENG; Tel: +86-13880745178; E-mail: 42881697@qq.com
DOI: 10.1016/S1003-6326(20)65228-1

explain pyrite depression by cyanide. WANG and FORSSBERG [8] found that cyanide was preferentially adsorbed on pyrite surface as iron cyanide compounds, inhibiting the chemisorption and oxidation of xanthate on pyrite and pyrite flotation. However, de WET et al [9] suggested that cyanide hindered the electrochemical activities and reduced the mixed potential of pyrite surface, which prevented the oxidation of xanthate to dixanthogen and then depressed pyrite flotation. Recently, GUO et al [10] have confirmed that the preferential adsorption of cyanide on pyrite as ferricyanide species rather than the decrease of pyrite redox potential was mainly responsible for pyrite depression by cyanide. When pyrite is activated by copper ions, cyanide acts as a deactivating agent, which removes cuprous ions from activated pyrite surface via the formation of strong cuprous cyanide complexes such as $Cu(CN)_3^{2-}$ and $Cu(CN)_4^{3-}$ by selectively dissolving cuprous-xanthates, -sulfides and -oxides [11]. When cyanide and copper ions co-exist, the depression effect of cuprous cyanide on pyrite is dependent on the redox potential and CN/Cu mole ratio in solution. As demonstrated by GUO and PENG [12], a reducing environment promotes the copper uptake and formation of copper sulfide on pyrite in copper cyanide solution, which may activate pyrite instead of depressing it, whilst at a high CN/Cu mole ratio, cyanide dissolves the formed copper sulfide, which is beneficial to pyrite depression.

To restore the floatability of pyrite depressed by cyanide, some activators may be used. LV et al [13] and YANG et al [14] used oxidizing agents such as sodium hypochlorite and hydrogen peroxide to activate the flotation of cyanide-depressed pyrite. The activation mechanism was attributed to the oxidation of cyanide to cyanate which eliminated the depression effect of cyanide on pyrite flotation. REDDY et al [15] used formaldehyde to activate the flotation of cyanide-depressed sphalerite, and found that formaldehyde could react with zinc cyanide to form cyanohydrins and desorb the cyanide layer from sphalerite surface, resulting in improved sphalerite flotation. However, they found that formaldehyde was inefficient to activate the flotation of cyanide-depressed pyrite because iron cyanide compounds on pyrite were too stable to be removed by formaldehyde.

It has been reported that sodium sulfide is used to activate the flotation of cyanide-depressed pyrite and some other oxide base metal minerals [1,16−18]. However, few studies have been carried out to underline the effect of sodium sulfide in this system. In the current study, pyrite was depressed in chalcocite flotation by cyanide and the depressed pyrite was then floated with the addition of sodium sulfide. The activation mechanism of sodium sulfide on cyanide-depressed pyrite was studied by electrochemical measurements. Together with the previous study [3], this study may provide new perspectives on the flotation enhancement of cyanide-depressed pyrite.

2 Experimental

2.1 Materials

The chalcocite and pyrite pure minerals were purchased from GEO Discoveries, Australia. They were both crushed in laboratory, and 0.71−3.35 mm fractions were collected from the crushed material. Elemental analysis and X-ray powder diffraction results showed that the pyrite and chalcocite purities were 96.0 wt.% and 96.4 wt.%, respectively. The crushed samples were kept in a refrigerator at −20 °C to eliminate the surface oxidation.

RTA11A (dithiocarbamate) was used as the chalcocite flotation collector, potassium amyl xanthate (PAX) was used as the pyrite flotation collector, and DSF004 (an aliphatic alcohol) was used as the frother. They were all of industrial purity and were used directly. Other chemicals were all analytical reagent grade. Deionized water (DI), with a resistivity of 18 MΩ/cm, was used in all experiments.

2.2 Methods

2.2.1 Flotation tests

10 g chalcocite and 90 g pyrite were mixed with 100 mL water and ground to 80 wt.% particles less than 106 μm in a rod mill for 4.8 min using stainless steel grinding media. Then the pulp was added to a 1.5 L flotation cell and conditioned with lime and sodium cyanide as pyrite depressants and 12 g/t RTD11A as chalcocite collector and 30 g/t DSF004 as frother. Each reagent was conditioned for 2 min. Four chalcocite concentrates were collected at an air flow rate of 6 L/min with flotation time of 1, 2, 3 and 4 min for each one.

After chalcocite flotation, sodium sulfide (if needed), PAX (if needed) and 30 g/t DSF004 were added to chalcocite tailing and conditioned for 2 min before pyrite flotation. The natural pH in pyrite flotation without the addition of sodium sulfide was 9. When sodium sulfide was added, HCl solution with a concentration of 1 mmol/L was added to maintain pH 9. Four pyrite flotation concentrates were collected in 1, 2, 3 and 4 min for each one. All the chalcocite and pyrite flotation concentrates and tailings were dried, weighted and assayed for chalcocite and pyrite grades and recoveries calculation.

2.2.2 Electrochemical measurements

In this work, cyclic voltammetry (CV) measurements were conducted to understand the interaction of PAX and Na_2S with cyanide-depressed pyrite. The experiment was performed with CHI 920D scanning electrochemical microscope (CH Instruments, Inc., USA) with a conventional three-electrode electrochemical cell. A double-layer wall glass reactor was used as the electrochemical cell with an effective volume of 200 mL. A Ag/AgCl electrode in 3 mol/L KCl electrolyte, a platinum plate electrode with a surface area of 1 cm^2 and the polished pyrite electrode were used as the reference, counter and working electrodes, respectively. Potentials were measured against the Ag/AgCl reference electrode which has a potential of 220 mV against a standard hydrogen electrode (SHE).

The experiments were conducted in air. Before each test, the surface of pyrite electrode was renewed by wet polishing using 1200 grit silicon carbide paper and rinsed with deionized water several times. Open circuit potential (OCP) sweep was conducted before each CV experiment which commenced when the OCP was stabilized (after approximately 10 min). In CV studies, cycles were performed from the OCP to 600 mV (a positive-going potential scan), then to −800 mV (a negative-going potential scan) and then back to the OCP at a scan rate of 20 mV/s. Four cycles were performed for each test and the second cycle was adopted because the shape and the peak intensity of oxidized or reduced species became stable since the second scan.

Experiments were performed in the absence and presence of sodium cyanide, sodium sulfide and PAX, individually and in combination. The reagent was added in the order of sodium cyanide, sodium sulfide (if needed) and PAX (if needed) according to the flotation procedure. Pyrite electrode was conditioned for 15 min in electrolyte solution after the addition of each reagent to reach the adsorption equilibrium before the electrochemical measurement. The background electrolyte was 0.1 mol/L potassium perchlorate ($KClO_4$) solution and the pH was adjusted to 9 with 1 mol/L KOH solution [19].

3 Results and discussion

3.1 Flotation

Chalcocite flotation was conducted first with RTD11A as the collector while pyrite was depressed. Figure 1 shows copper grade as a function of copper recovery from the flotation at pH 10. When the pH was adjusted by lime without the addition of cyanide, the flotation produced about 96.4% of copper recovery at about 45.1% of copper grade after 10 min flotation. Pyrite recovery was about 11.6%. This is different from the previous study [3] where pyrite was completely depressed by lime at pH 10 in chalcopyrite flotation. It has been reported that chalcocite is more electrochemically active than chalcopyrite, and the galvanic interaction is stronger between chalcocite and pyrite than between chalcopyrite and pyrite [6]. Therefore, more copper ions are available from the chalcocite−pyrite system to activate pyrite, resulting in more difficult depression of pyrite in chalcocite flotation by lime.

Figure 1 also shows that the addition of 200 g/t NaCN increased copper grade significantly to 57.3%

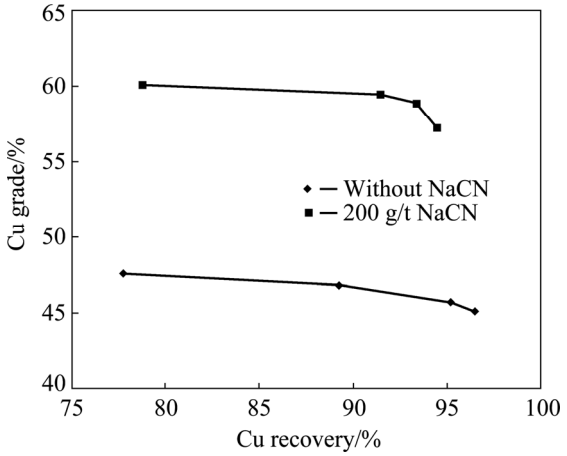

Fig. 1 Copper grade as function of copper recovery in chalcocite flotation with pyrite depressed at pH 10

while decreasing copper recovery slightly to 94.2%. Pyrite was completely depressed with about 2.6% of recovery. GUO et al [20] demonstrated that the activation of copper ions on pyrite flotation could be mitigated by cyanide due to the formation of soluble cuprous cyanide complexes.

After chalcocite flotation, pyrite flotation was conducted to recover the pyrite depressed by cyanide. In the previous study [20], PAX, Na_2S and their combination were adopted to activate lime-depressed pyrite. In the current study, these approaches were taken to activate cyanide-depressed pyrite and the results are shown in Fig. 2. As can be seen, pyrite recovery was only about 2.2% in the absence of Na_2S and PAX due to the previous depression in chalcocite flotation. However, the presence of either Na_2S or PAX was able to promote sufficient pyrite flotation. For example, pyrite recovery increased to 42.6% and 68.3% at 15 g/t and 30 g/t PAX, respectively, and 29.8%, 48.7%, 55.4% and 63.5% at 120, 240, 360 and 480 g/t Na_2S, respectively. This indicates that hydrophobic products formed on pyrite surface in the presence of Na_2S or PAX. Figure 2 also shows that the combination of Na_2S and PAX enhanced pyrite flotation. As can be seen, pyrite recovery reached 90% at 30 g/t PAX and 480 g/t Na_2S.

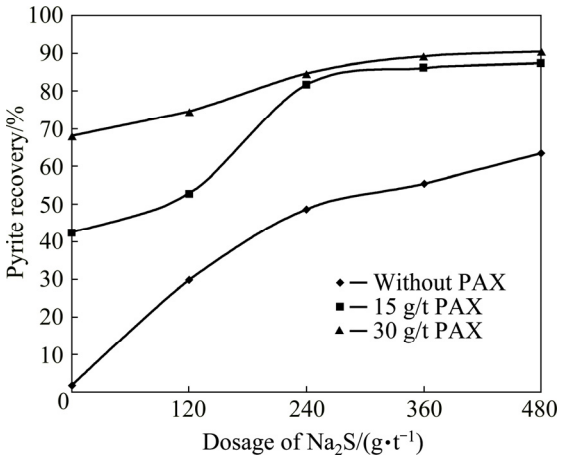

Fig. 2 Effect of PAX, Na_2S and their combination on flotation of pyrite depressed by cyanide in chalcocite flotation at pH 9

Both Na_2S and PAX are reducing agents, indicating that activation on cyanide-depressed pyrite may involve electrochemical reactions. In the following section, the electrochemical reactions of Na_2S and PAX with cyanide-depressed pyrite were investigated.

3.2 Electrochemical analysis

Cyclic voltammetry (CV) was used to understand the reactions of Na_2S and PAX with cyanide-depressed pyrite. Firstly, the CV curve of pyrite electrode in 0.1 mol/L potassium perchlorate background solution at pH 9 was obtained. As shown in Fig. 3, there were two anodic peaks (A1 and A2) on the positive-going sweep and two cathodic peaks (C1 and C2) on the negative-going sweep in the CV curve of pyrite electrode. The anodic peak A1 was attributed to the oxidation of pyrite resulting in the formation of ferric hydroxide, and a sulfur-rich sublayer which may be elemental sulfur (S^0), polysulfides (FeS_n) and metal-deficient sulfide ($Fe_{1-x}S_2$) [21]. The surface reaction for A_1 is shown in Eq. (1).

$$FeS_2+3H_2O=Fe(OH)_3+2S^0+3H^++3e \quad (1)$$

Peak A2 was due to the aggressive oxidation of pyrite to ferric hydroxide and sulfate as shown in Eq. (2) when the upper potential increases to 600 mV [22].

$$FeS_2+11H_2O=Fe(OH)_3+2SO_4^{2-}+19H^++15e \quad (2)$$

The cathodic peaks resulted from the reduction of the oxidation species formed during the anodic process. Peak C1 was attributed to the reduction of ferric hydroxide to ferrous hydroxide while peak C2 was related to the reduction of elemental sulfur to HS^- [10,17]. The reactions responsible for peaks C1 and C2 are shown in Eqs. (3) and (4), respectively.

$$Fe(OH)_3+e=Fe(OH)_2+OH^- \quad (3)$$

$$S^0+H_2O+2e=HS^-+OH^- \quad (4)$$

Figure 4 shows the CV curves of pyrite electrode in the presence of 0.2 mmol/L NaCN,

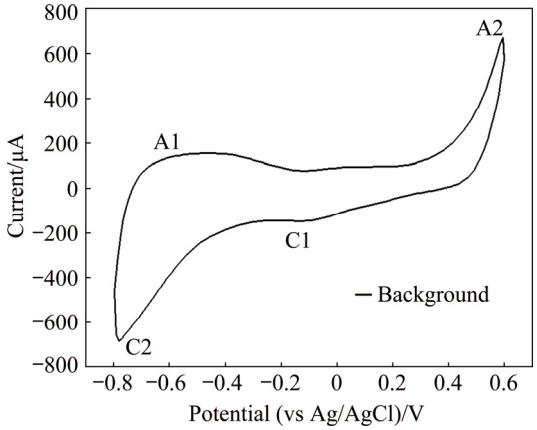

Fig. 3 CV curve of pyrite electrode in background solution at pH 9

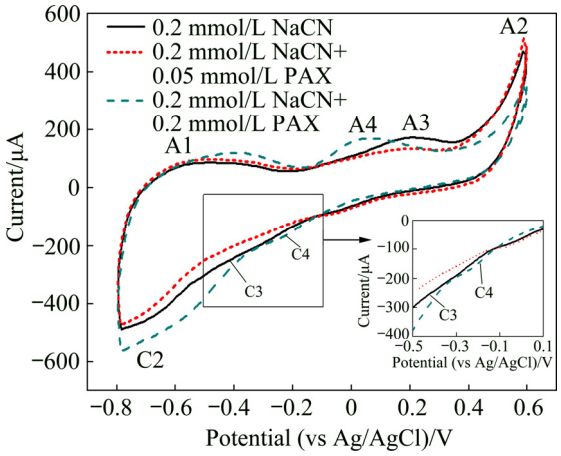

Fig. 4 CV curves of pyrite electrode in the presence of 0.2 mmol/L NaCN without and with addition of 0.05 or 0.2 mmol/L PAX at pH 9

without and with the addition of 0.05 or 0.2 mmol/L PAX. In the presence of NaCN, an anodic peak A3 and a cathodic peak C3 appeared on the CV curve of pyrite electrode. Peak A3 was due to the formation of ferricyanide $Fe(CN)_6^{3-}$ on pyrite surface which was confirmed by GUO et al [10] using surface enhanced Raman spectroscopy. This reaction is shown in Eq. (5). Peak C3 commenced at −0.35 mV and resulted from the reduction of $Fe(CN)_6^{3-}$ to $Fe(CN)_6^{4-}$ as shown in Eq. (6) [23].

$$FeS_2+8CN^-=Fe(CN)_6^{3-}+2SCN^-+3e \quad (5)$$

$$Fe(CN)_6^{3-}+e=Fe(CN)_6^{4-} \quad (6)$$

Peaks A3 and C3 which indicate the formation of $Fe(CN)_6^{3-}$ and its reduction, respectively, in the presence of 0.2 mmol/L NaCN both weakened or even disappeared after the addition of 0.05 or 0.2 mmol/L PAX. After the addition of 0.2 mmol/L PAX, two new peaks A4 and C4 appeared on the CV curve of pyrite electrode in the presence of 0.2 mmol/L NaCN. These two new peaks were attributed to the oxidation of xanthate to dixanthogen as shown in Eq. (7) and its reduction to xanthate [24−27].

$$2X^-=X_2+2e \quad (7)$$

Figure 4 clearly indicates that the displacement of cyanide species by PAX can take place on pyrite surface, which means that the cyanide species formed on pyrite surface can be removed by PAX, accompanied by the formation of dixanthogen at a higher PAX concentration. WANG et al [28] indicated that insoluble hydroxyl ferric xanthate ($Fe(OH)X_2$) could be formed in the weakly acidic to alkaline pH range. The formation of insoluble $Fe(OH)X_2$ may drive the displacement of ferricyanide ($Fe(CN)_6^{3-}$) from pyrite surface by PAX as

$$Fe(CN)_6^{3-}+OH^-+2X^-=Fe(OH)X_2+6CN^- \quad (8)$$

The Gibbs free energy change (Δ_rG) for Eq. (8) can be calculated as follows:

$$\Delta_rG=\Delta_rG^{\Theta}+RT\ln\frac{[Fe(OH)X_2][CN^-]^6}{[Fe(CN)_6^{3-}][OH^-][X^-]^2}=$$
$$-RT\ln\frac{1}{K_{Fe(CN)_6^{3-}}K_{spFe(OH)X_2}}+$$
$$RT\ln\frac{[Fe(OH)X_2][CN^-]^6}{[Fe(CN)_6^{3-}][OH^-][X^-]^2} \quad (9)$$

where R and T are the ideal gas constant of 8.314 J/(mol·K) and thermodynamic temperature of 298.15 K, respectively. The stability constant (K) of $Fe(CN)_6^{3-}$ is $10^{43.6}$ and the solubility product constant (K_{sp}) of $Fe(OH)X_2$ is $10^{-35.5}$ [28]. At pH 9, OH^- concentration is 10^{-5} mol/L. Assuming that the activities of $Fe(CN)_6^{3-}$ and $Fe(OH)X_2$ are unity at pyrite−aqueous interface [10], the calculated Gibbs free energy change Δ_rG for Eq. (8) is −9.7 kJ/mol at 0.2 mmol/L NaCN and 0.2 mmol/L PAX. The negative Gibbs free energy change for Eq. (8) means that the ferricyanide $Fe(CN)_6^{3-}$ on pyrite surface could be displaced by PAX at a high concentration. After $Fe(CN)_6^{3-}$ on pyrite surface is displaced by PAX, PAX may be oxidized to dixanthogen.

The displacement of ferricyanide and formation of dixanthogen may be responsible for the flotation of pyrite depressed by cyanide in the presence of PAX as shown in Fig. 2.

Figure 5 shows the CV curves of pyrite electrode in the presence of 0.2 mmol/L NaCN without and with the addition of 0.1 or 0.4 mmol/L Na_2S at pH 9. It can be seen that peaks A3 and C3 which indicate the formation of $Fe(CN)_6^{3-}$ and its reduction, respectively, both weakened or even disappeared after the addition of 0.1 or 0.4 mmol/L Na_2S. In addition, the addition of Na_2S brought forth a new anodic peak A5 and a new cathodic peak C5 on the CV curve of pyrite electrode. Peak A5 is attributed to the oxidation of sulfide ions (S^{2-}) to elemental sulfur (S^0) as shown in Eq. (10) and the S^0 species may react with a subtending disulfide

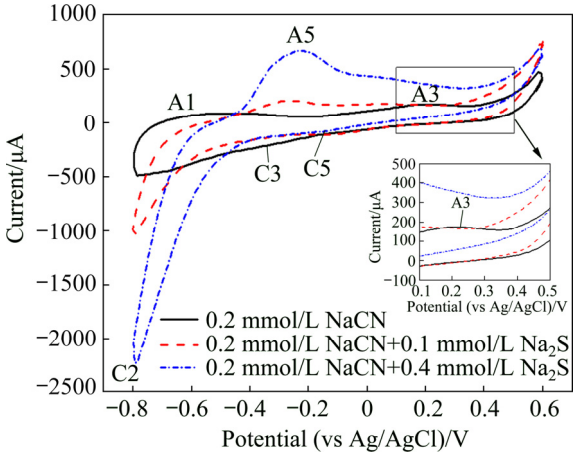

Fig. 5 CV curves of pyrite electrode in the presence of 0.2 mmol/L NaCN without and with addition of 0.1 or 0.4 mmol/L Na_2S at pH 9

layer (S_2^{2-}) on pyrite surface to produce polysulfide (S_n^{2-}) [29]. Peak C5 is attributed to the reduction of $Fe(CN)_6^{3-}$ on pyrite surface, resulting in the formation of FeS in the presence of sulfide ions as shown in Eq. (11) [30,31].

$$S^{2-}=S^0+2e \quad (10)$$

$$Fe(CN)_6^{3-}+S^{2-}+e=FeS+6CN^- \quad (11)$$

The current intensity of peak A5 in Fig. 5 increased with the increase of Na_2S concentration, which suggests the formation of more elemental sulfur/polysulfide S^0/S_n^{2-} on pyrite surface at a higher Na_2S concentration. The current intensity of peak C2 which was attributed to the reduction of elemental sulfur to HS^- also increased with the increase of Na_2S concentration. This also suggests that more elemental sulfur/polysulfide formed on pyrite surface at a higher Na_2S concentration as reported by WALKER et al [32]. It was noted that the current intensity of peak C5 with the addition of 0.4 mmol/L Na_2S was slightly lower than that with the addition of 0.1 mmol/L Na_2S. This might be because less $Fe(CN)_6^{3-}$ could be formed on pyrite surface in the presence of cyanide when a higher concentration of Na_2S was added.

Based on the above oxidation of sulfide ions (S^{2-}) and reduction of $Fe(CN)_6^{3-}$, the overall redox reaction of Na_2S with cyanide-depressed pyrite can be expressed as

$$2Fe(CN)_6^{3-}+3S^{2-}=2FeS+S^0+12CN^- \quad (12)$$

The species in Eq. (12) and their standard free energies of formation are shown in Table 1. The Gibbs' free energy change ($\Delta_r G$) of Eq. (12) is −25.58 kJ/mol, a negative value, confirming that this reaction would be thermodynamically possible. Equation (12) may be responsible for the flotation of cyanide-depressed pyrite in the presence of Na_2S as shown in Fig. 2.

Table 1 Fe−S−CN species and their standard free energies of formation

Species	$\Delta_f G^{\Theta}$/(kJ·mol^{-1})	Ref.
$Fe(CN)_6^{3-}$	694.92	[10]
S^{2-}	85.8	[33]
FeS	−113.4	[34]
S^0	0	[34]
CN^-	172.38	[10]

Figure 6 shows the CV curves of pyrite electrode in the presence of 0.2 mmol/L NaCN with the addition of 0.4 mmol/L Na_2S and 0.2 mmol/L PAX individually and in combination at pH 9. Peaks A4 and A5 which are responsible for the formation of dixanthogen due to the oxidation of xanthate and the formation of elemental sulfur/polysulfide due to the oxidation of sulfide ions on pyrite surface, respectively, both appeared on the positive-going scan of pyrite electrode when 0.4 mmol/L Na_2S and 0.2 mmol/L PAX were added in combination. These hydrophobic products may render the pyrite surface strongly hydrophobic. Clearly, the addition of PAX and Na_2S at the same time can facilitate the flotation of pyrite previously depressed by cyanide in chalcocite flotation.

Figure 7 illustrates the surface chemistry change of cyanide-depressed pyrite in the presence

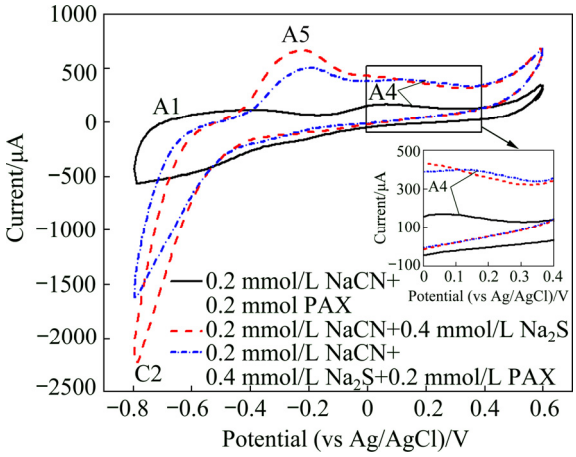

Fig. 6 CV curves of pyrite electrode in the presence of 0.2 mmol/L NaCN with addition of 0.4 mmol/L Na_2S and 0.2 mmol/L PAX individually and in combination at pH 9

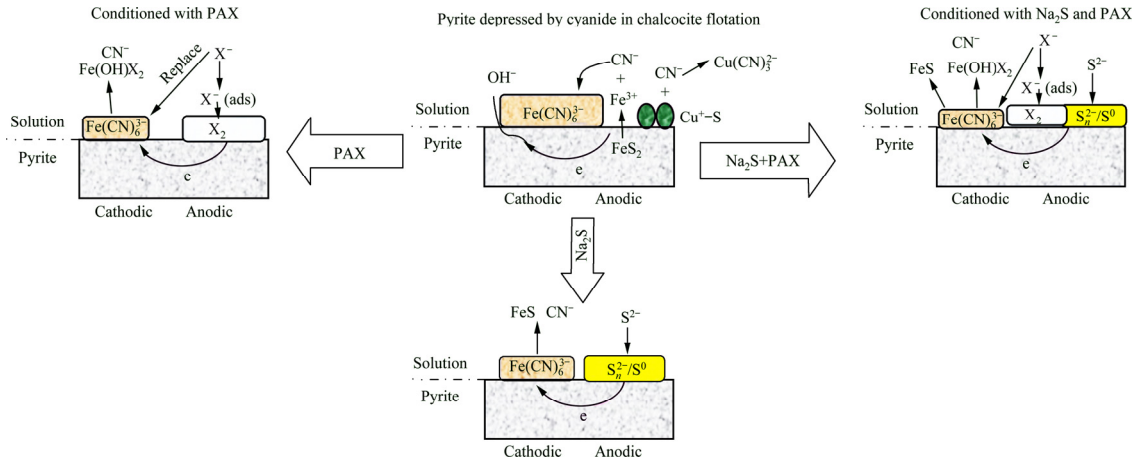

Fig. 7 Possible reaction mechanisms of cyanide-depressed pyrite with Na_2S, PAX and their combination

of Na_2S, PAX and their combination. In the presence of PAX, the displacement of ferricyanide by xanthate ions and the formation of dixanthogen may be responsible for the flotation of cyanide-depressed pyrite at a high concentration of PAX [8]. Unlike PAX, Na_2S promotes pyrite flotation through the reduction of ferricyanide species and the formation of elemental sulfur and polysulfide. The addition of PAX and Na_2S at the same time may induce superior pyrite flotation as a result of the combined actions from PAX and Na_2S.

4 Conclusions

(1) Both PAX and Na_2S can be used to float pyrite depressed by cyanide in chalcocite flotation. However, their combination is better than each of them to improve the flotation of cyanide-depressed pyrite.

(2) Different mechanisms could be used to underline the flotation enhancement of cyanide-depressed pyrite by PAX and Na_2S. PAX can compete with cyanide and be oxidized to dixanthogen on pyrite surface, whereas Na_2S can reduce the ferricyanide species on pyrite with the formation of elemental sulfur S^0 and polysulfide S_n^{2-}. Therefore, the hydrophobicity and floatability of pyrite can be improved by both PAX and Na_2S. Moreover, the application of PAX and Na_2S at the same time can further enhance the hydrophobicity and floatability of pyrite because of a synergistic effect between PAX and Na_2S.

References

[1] ZHENG X, MANTON. A potential application of collectorless flotation in a copper/gold operation [J]. Minerals Engineering, 2010, 23: 895−902.

[2] BULATOVIC S M. Flotation behaviour of gold during processing of porphyry copper−gold ores and refractory gold-bearing sulphides [J]. Minerals Engineering, 1997, 10: 895−908.

[3] CAO Z, CHEN X, PENG Y. The role of sodium sulfide in the flotation of pyrite depressed in chalcopyrite flotation [J]. Minerals Engineering, 2018, 119: 93−98.

[4] LASCELLES D, FINCH J A. Quantifying accidental activation, Part I: Cu ion production [J]. Minerals Engineering, 2002, 15: 567−571.

[5] WONG G, LASCELLES D, FINCH J A. Quantifying accidental activation, Part II: Cu activation of pyrite [J]. Minerals Engineering, 2002, 15: 573−576.

[6] CHEN X, PENG Y, BRADSHAW D. The separation of chalcopyrite and chalcocite from pyrite in cleaner flotation after regrinding [J]. Minerals Engineering, 2014, 58: 64−72.

[7] BULATOVIC S, WYSLOUZIL D M. Selection and evaluation of different depressants systems for flotation of complex sulphide ores [J]. Minerals Engineering, 1995, 8: 63−76.

[8] WANG X H, FORSSBERG K S E. The solution electrochemistry of sulfide−xanthate−cyanide systems in sulfide mineral flotation [J]. Minerals Engineering, 1996, 9: 527−546.

[9] de WET J R, PISTORIUS P C, SANDENBERGH R F. The influence of cyanide on pyrite flotation from gold leach residues with sodium isobutyl xanthate [J]. International Journal of Mineral Processing, 1997, 49: 149−169.

[10] GUO B, PENG Y, PARKER G. Electrochemical and spectroscopic studies of pyrite–cyanide interactions in relation to the depression of pyrite flotation [J]. Minerals Engineering, 2016, 92: 78−85.

[11] PRESTIDGE C A, SKINNER W M, RALSTON J, SMART R S C. Copper(II) activation and cyanide deactivation of zinc sulphide under mildly alkaline conditions [J]. Applied Surface Science, 1997, 108: 333−344.

[12] GUO B, PENG Y. The interaction between copper species and pyrite surfaces in copper cyanide solutions [J]. International Journal of Mineral Processing, 2017, 158: 85−92.

[13] LV C C, DING J, QIAN P, LI Q C, YE S F, CHEN Y F. Comprehensive recovery of metals from cyanidation tailing [J]. Minerals Engineering, 2015, 70: 141−147.

[14] YANG X, HUANG X, QIU T. Recovery of zinc from

cyanide tailings by flotation [J]. Minerals Engineering, 2015, 84: 100−105.
[15] REDDY G S, REDDY C K, SEKHAR D M R, RAVINDRANATH K, CHULET M R. Effect of formaldehyde and nickel sulphate solutions on the activation of cyanide-depressed sphalerite [J]. Minerals Engineering, 1991, 4: 151−160.
[16] SEAMAN D R, LAUTEN R A, KLUCK G, STOITIS N. Usage of anionic dispersants to reduce the impact of clay particles in flotation of copper and gold at the Telfer mine [C]//Proceedings of the 11th Mill Operators' Conference. Hobart, Tasmania: AusIMM, 2012: 207−214.
[17] WANG Li, HU Guang-yan, SUN Wei, KHOSO S A, LIU Run-qing, ZHANG Xiang-feng. Selective flotation of smithsonite from dolomite by using novel mixed collector system [J]. Transactions of Nonferrous Metals Society of China, 2019, 29: 1082−1089.
[18] YIN Wan-zhong, SUN Qian-yu, LI Dong, TANG Yuan, FU Ya-feng, YAO Jin. Mechanism and application on sulphidizing flotation of copper oxide with combined collectors [J]. Transactions of Nonferrous Metals Society of China, 2019, 29: 178−185.
[19] WANG X H. Interfacial electrochemistry of pyrite oxidation and flotation I: Effect of borate on pyrite surface oxidation [J]. Journal of Colloid and Interface Science, 1996, 178: 628−637.
[20] GUO B, PENG Y, ESPINOSA GOMEZ R. Cyanide chemistry and its effect on mineral flotation [J]. Minerals Engineering, 2014, 66−68: 25−32.
[21] MU Y, PENG Y, LAUTEN R A. The depression of copper-activated pyrite in flotation by biopolymers with different compositions [J]. Minerals Engineering, 2016, 96−97: 113−122.
[22] MILLER J D, PLESSIS R D, KOTYLAR D G, ZHU X, SIMMONS G L. The low-potential hydrophobic state of pyrite in amyl xanthate flotation with nitrogen [J]. International Journal of Mineral Processing, 2002, 67: 1−15.
[23] KAWIAK J, JEDRAL T, GALUS Z. A reconsideration of the kinetic data for the Fe(CN)63-/Fe(CN)64-system [J]. Journal of Electroanalytical Chemistry, 1983, 145: 163−171.
[24] LÓPEZ VALDIVIESO A, SÁNCHEZ LÓPEZ A A, SONG S. On the cathodic reaction coupled with the oxidation of xanthates at the pyrite/aqueous solution interface [J]. International Journal of Mineral Processing, 2005, 77: 154−164.
[25] BULUT G, ATAK S. Role of dixanthogen on pyrite flotation: Solubility, adsorption studies and Eh, FTIR measurements [J]. Minerals & Metallurgical Processing, 2002, 19: 81−86.
[26] WANG X H. Interfacial electrochemistry of pyrite oxidation and flotation II: FTIR studies of xanthate adsorption on pyrite surface in neutral pH solutions [J]. Journal of Colloid and Interface Science, 1995, 171: 413−428.
[27] JIANG C L, WANG X H, PAREKH B K, LEONARD J W. The surface and solution chemistry of pyrite flotation with xanthate in the presence of iron ions [J]. Colloids and Surfaces A: Physicochemical and Engineering Aspects, 1998, 136: 51−62.
[28] WANG X, FORSSBERG K S E, BOLIN N J. Thermodynamic calculations on iron-containing sulphide mineral flotation systems I: The stability of iron-xanthates [J]. International Journal of Mineral Processing, 1989, 27: 1−19.
[29] EJTEMAEI M, NGUYEN A V. Characterisation of sphalerite and pyrite surfaces activated by copper sulphate [J]. Minerals Engineering, 2017, 100: 223−232.
[30] LAWRENCE N S, THOMPSON M, PRADO C, JIANG L, JONES T G J, COMPTON R G. Amperometric detection of sulfide at a boron doped diamond electrode: The electrocatalytic reaction of sulfide with ferricyanide in aqueous solution [J]. Electroanalysis, 2002, 14: 499−504.
[31] LIU S, LI M, LI S, LI H, YAN L. Synthesis and adsorption/photocatalysis performance of pyrite FeS_2 [J]. Applied Surface Science, 2013, 268: 213−217.
[32] WALKER G W, WALTERS C P, RICHARDSON P E. Hydrophobic effects of sulfur and xanthate on metal and mineral surfaces [J]. International Journal of Mineral Processing, 1986, 18: 118−137.
[33] GUO B. Electrodeposition on pyrite from copper(I) cyanide electrolyte [J]. RSC Advance, 2016, 6: 2183−2190.
[34] RICKARD D, LUTHER III G W. Chemistry of iron sulfides [J]. Chemical Reviews, 2007, 107: 514−552.

硫化钠对氰化抑制黄铁矿浮选的作用机理

曹 钊[1,2,3]，王 鹏[1]，张文博[1]，曾小波[4]，曹永丹[1]

1. 内蒙古科技大学 矿业研究院，包头 014010；2. 广东省资源综合利用研究所，广州 510650；
3. 稀有金属分离与综合利用国家重点实验室，广州 510650；
4. 中国地质科学院 矿产综合利用研究所，成都 610041

摘 要：通过浮选试验及电化学测试，研究戊基黄原酸钾(PAX)为捕收剂时硫化钠对氰化抑制黄铁矿浮选的作用机理。浮选结果表明，PAX 和硫化钠单独使用时都可以提高氰化抑制黄铁矿的浮选回收率，但二者组合使用时对回收率的提升效果更加显著。电化学结果表明，PAX 与硫化钠在氰化抑制黄铁矿的表面具有不同的作用形式，PAX 可取代黄铁矿表面的氰根并以双黄药形式吸附于黄铁矿表面，导致黄铁矿表面疏水及可浮；而硫化钠可还原黄铁矿表面的铁氰化物并在黄铁矿表面生成单质硫和多硫化物，进而使黄铁矿表面疏水。组合使用时由于二者的协同作用会进一步提高黄铁矿的浮选回收率。

关键词：黄铁矿；辉铜矿；浮选；氰化物；抑制；硫化钠

(Edited by Xiang-qun LI)